

# UC San Diego

## UC San Diego Previously Published Works

### Title

MicroRNA-mediated regulation of extracellular matrix formation modulates somatic cell reprogramming

### Permalink

<https://escholarship.org/uc/item/91x8v2t9>

### Journal

RNA, 20(12)

### ISSN

1355-8382

### Authors

Li, Zhonghan  
Dang, Jason  
Chang, Kung-Yen  
[et al.](#)

### Publication Date

2014-12-01

### DOI

10.1261/rna.043745.113

Peer reviewed

---

# MicroRNA-mediated regulation of extracellular matrix formation modulates somatic cell reprogramming

---

ZHONGHAN LI,<sup>1,4</sup> JASON DANG,<sup>1,2,4</sup> KUNG-YEN CHANG,<sup>1,3</sup> and TARIQ M. RANA<sup>1,3</sup>

<sup>1</sup>Program for RNA Biology, Sanford-Burnham Medical Research Institute, La Jolla, California 92037, USA

<sup>2</sup>Department of Bioengineering, University of California San Diego, La Jolla, California 92093, USA

<sup>3</sup>Department of Pediatrics, University of California San Diego School of Medicine, La Jolla, California 92093, USA

## ABSTRACT

Somatic cells can be reprogrammed to reach an embryonic stem cell-like state by overexpression of defined factors. Recent studies have greatly improved the efficiency of the reprogramming process but the underlying mechanisms regulating the transition from a somatic to a pluripotent state are still relatively unknown. MicroRNAs (miRs) are small noncoding RNAs that primarily regulate target gene expression post-transcriptionally. Here we present a systematic and comprehensive study of microRNAs in mouse embryonic fibroblasts (MEFs) during the early stage of cell fate decisions and reprogramming to a pluripotent state, in which significant transcriptional and epigenetic changes occur. One microRNA found to be highly induced during this stage of reprogramming, miR-135b, targeted the expression of extracellular matrix (ECM) genes including *Wisp1* and *Igfbp5*. *Wisp1* was shown to be a key regulator of additional ECM genes that serve as barriers to reprogramming. Regulation of *Wisp1* is likely mediated through biglycan, a glycoprotein highly expressed in MEFs that is silenced in reprogrammed cells. Collectively, this report reveals a novel link between microRNA-mediated regulation of ECM formation and somatic cell reprogramming, and demonstrates that microRNAs are powerful tools to dissect the intracellular and extracellular molecular mechanisms of reprogramming.

**Keywords:** ECM; iPS; miRNA

## INTRODUCTION

Since the first report that mouse fibroblasts can be reprogrammed into a pluripotent state reminiscent of embryonic stem cells (termed induced pluripotent stem cells, iPSC) (Takahashi and Yamanaka 2006), this phenomenon has been confirmed using many different mouse and human cell types (Takahashi et al. 2007; Wernig et al. 2007; Yu et al. 2007; Lowry et al. 2008; Nakagawa et al. 2008; Park et al. 2008). One of the challenges for the development of successful application of iPSCs for medical purposes is their low reprogramming efficiency. Several approaches have been applied to enhance induced reprogramming efficiency, including strategies focusing on the use of mRNA (Warren et al. 2010); small molecules (Silva et al. 2008; Ying et al. 2008; Ichida et al. 2009; Maherali and Hochedlinger 2009; Nichols et al. 2009; Yang et al. 2011b; Zhu et al. 2011; Li and Rana 2012); and miRNAs (Judson et al. 2009; Melton et al. 2010; Choi et al. 2011; Kim et al. 2011; Li et al. 2011; Liao et al. 2011; Lipchina et al. 2011; Pfaff et al. 2011; Subramanyam et al.

2011; Yang et al. 2011a; Li and He 2012; Yang and Rana 2013). Intriguingly, a recent study reported in which somatic cells were completely reprogrammed to a pluripotent state only using a combination of seven small molecules (Hou et al. 2013). However, the molecular mechanisms by which the four factors are able to reprogram somatic cells remain largely unknown.

A number of studies suggest that somatic cell reprogramming is a complex and dynamic process involving many different transcriptional and epigenetic changes. Systematic analysis of the promoters targeted by overexpression of the four reprogramming factors has demonstrated that expression of the factor target genes is similar in iPSCs and mouse embryonic stem (mES) cells, and is altered in some partially reprogrammed cells (Sridharan et al. 2009). The p53 pathway has been identified as one primary barrier to reprogramming (Banito et al. 2009; Hong et al. 2009; Kawamura et al. 2009; Li et al. 2009a; Utikal et al. 2009). Chemical screening has also discovered that inhibition of TGF $\beta$  signaling significantly enhances reprogramming (Ichida et al. 2009) and that some inhibitors of this pathway can replace the Sox2 transgene in

---

<sup>4</sup>These authors contributed equally to this work.

Corresponding author: trana@ucsd.edu

Article published online ahead of print. Article and publication date are at <http://www.rnajournal.org/cgi/doi/10.1261/rna.043745.113>. Freely available online through the RNA Open Access option.

© 2014 Li et al. This article, published in RNA, is available under a Creative Commons License (Attribution-NonCommercial 4.0 International), as described at <http://creativecommons.org/licenses/by-nc/4.0/>.

inducing expression of Nanog, a transcription factor crucial for ESC pluripotency (Maherali and Hochedlinger 2009). In addition, it was suggested that a mesenchymal-to-epithelial transition (MET) is a key step that takes place at an early stage of reprogramming (Li et al. 2010; Samavarchi-Tehrani et al. 2010). During reprogramming, expression of markers on the initial somatic cell, such as mouse embryonic fibroblasts (MEFs), are down-regulated and characteristic mES markers, such as alkaline phosphatase, SSEA1, Nanog, and endogenous Oct4 become expressed (Brambrink et al. 2008; Stadtfeld et al. 2008). Interestingly, the cellular origin of the iPSCs apparently influences their ability to retain an epigenetic “memory” of the originating cell, a property that is gradually lost through continuous passaging of iPSCs. It has been shown that >92% of the monoclonal pre-B cells could reach a fully reprogrammed state when cultured as monoclonal for extended periods (Hanna et al. 2009), while <0.1% were fully reprogrammed when starting with a mixed population (Sridharan et al. 2009). In addition, recent reports suggest that a privileged somatic state exists in which cells with accelerated cell cycles overcome the stochastic nature of reprogramming and efficiently generate iPSC (Guo et al. 2014). However, iPSCs do not seem to have a generic epigenetic state that could clearly define the fully reprogrammed state (Carey et al. 2011). Highlighting the importance of the epigenetic state during reprogramming, knockdown of the ubiquitously expressed chromatin remodeling Mbd3/NuRD repressor complexes in somatic cells has been shown to greatly enhance iPSC induction to nearly 100% efficiency (Rais et al. 2013). Despite this progress, there remains only limited information on the mechanisms by which the four transgenes and other cellular factors reprogram MEFs to an undifferentiated or ES-like state. Recent functional genomics studies have provided insight into essential and barrier pathways involved in iPSC generation during various steps of reprogramming (Qin et al. 2014; Sakurai et al. 2014; Yang et al. 2014).

While significant progress is being made in understanding the intracellular signaling pathways governing somatic cell reprogramming, little is known about the extracellular events also associated with the reprogramming process. The extracellular matrix (ECM) is a multifunctional system that is involved in many stages of mammalian development (Sanes 1989; Adams and Watt 1993; Rozario and DeSimone 2010) and human disease progressions, including tumor formation (Kessenbrock et al. 2010; Bissell and Hines 2011). ECM is made of secreted polysaccharides and proteins that are organized into a well-defined complex structure surrounding the surface of cells that produce them. A variety of proteins and polysaccharides are involved in ECM, which could be divided into at least two groups: proteins with structural role, such as fibrous proteins and glycosaminoglycans; and proteins with regulatory role, including different growth factors (e.g., TGF $\beta$  and IGFs), matricellular proteins (CCN family proteins, IGFBPs, decorin, and biglycan), enzymes (metalloproteinases), and receptors (integrins). ECM plays a crucial

role in regulating various cellular behaviors and maintaining the identity and normal function of those cells (Kessenbrock et al. 2010; Bissell and Hines 2011). For embryonic stem cells, ECM components are essential for establishing the proper niche for long-term ES cell survival and self-renewal (Bendall et al. 2007; Peerani et al. 2007). Moreover, recent studies have shown that culture media supplemented with FGF2 can enhance iPSC induction through the regulation of collagen gene expression, thus bringing attention to the role of the microenvironment in reprogramming (Jiao et al. 2013). In fact, given the dramatic changes of both cellular morphology and functional characteristics during the course of reprogramming, potential iPSCs would need to establish their own niche for supporting their growth and colony formation. At the same time, successful iPSCs also need to exclude the effects brought by secreted ECM proteins from surrounding cells that are not reprogrammed. However, despite that iPSCs expressed a different set of ECM proteins from starting fibroblasts cells (Sridharan et al. 2009), little is known about the dynamic remodeling of ECMs during reprogramming. Understanding the molecular mechanisms that govern ECM remodeling during reprogramming would provide fundamental knowledge essential in efficiently creating and controlling various states of pluripotent stem cells.

MicroRNAs are 18–24 nucleotide long, single-stranded RNAs associated with a protein complex termed the RNA-induced silencing complex (RISC). Small RNAs are usually generated from noncoding regions of gene transcripts and function to suppress gene expression by translational repression and mRNA degradation (Ambros 2004; Chu and Rana 2006, 2007; Rana 2007; Djuranovic et al. 2011; Huntzinger and Izaurralde 2011). Recent work indicates that ES-specific microRNAs can enhance iPSC induction (Judson et al. 2009) and, specifically, that the hES miR-302 can antagonize the senescence response induced by four-factor expression in human fibroblasts (Banito et al. 2009). In addition, our recent findings suggest that the microRNA biogenesis machinery may be required for efficient reprogramming (Li et al. 2011), and microRNAs induced by OSKM are known to regulate several key pathways affecting reprogramming efficiency, including cell cycle control, the p53 pathway, TGF $\beta$  signaling, and MET (Choi et al. 2011; Li et al. 2011; Liao et al. 2011; Subramanyam et al. 2011; Yang et al. 2011a). Moreover, during somatic reprogramming, many microRNAs undergo small changes in expression in the early stages while only a select few microRNAs undergo large changes in expression in the later stages of reprogramming (Polo et al. 2012; Henzler et al. 2013). These data indicate a transition from a deterministic to stochastic process and suggest that microRNAs are regulated in a highly stage-dependent manner during reprogramming. Importantly, expression of microRNAs alone can fully reprogram fibroblasts to iPSCs (Anokye-Danso et al. 2011; Huntzinger and Izaurralde 2011; Miyoshi et al. 2011; Polo et al. 2012; Henzler et al. 2013). These findings clearly suggest that microRNAs play

crucial roles during the reprogramming process by targeting key barrier signaling networks. However, most studies to date have focused on intracellular signaling networks regulated by microRNAs, and the ability of microRNAs to influence critical cellular interactions with the microenvironmental niche during reprogramming has not yet been investigated.

Here, we performed a systematic analysis of expression of microRNAs and their potential target genes at an early stage of reprogramming, and identified a novel link between microRNAs, ECM formation, and reprogramming of MEFs. In particular, we found that microRNA-135b is highly induced and modulating its expression significantly affected the reprogramming process. Using genome-wide mRNA array analysis, we show that miR-135b controls expression of *Tgfb2*, *Igfbp5*, and *Wisp1*, the latter two genes encoding components of the MEF ECM. *Wisp1* was found to regulate the secretion of several ECM proteins including TGFBI (TGF- $\beta$  induced), IGFBP5 (insulin-like growth factor binding proteins-5), NOV (nephroblastoma overexpressed gene), and DKK2 (dickkopf homolog 2) proteins. Interestingly, the effects of *Wisp1* are mediated through biglycan, a glycoprotein that is highly expressed in MEFs and is incompletely silenced in reprogramming cells. Notably, knockdown or overexpression of biglycan enhanced or suppressed MEF reprogramming, respectively. Collectively, our results have identified a novel role for microRNA-mediated regulation of ECM formation in iPSC generation, and further, demonstrate that microRNAs can be powerful tools to dissect and understand the intracellular and extracellular molecular mechanisms of somatic cell reprogramming.

## RESULTS

### Systematic identification of highly regulated microRNAs during the early stages of reprogramming

We hypothesized that at different reprogramming stages, potential iPSCs may express unique “marker signatures” of microRNAs that regulate how the cells reach a fully reprogrammed stage. Previous findings indicate that reprogramming of MEFs is accompanied by sequential modulation of somatic cell and stem cell markers at different reprogramming stages (Brambrink et al. 2008; Stadtfeld et al. 2008), which can be used to track the process. These markers include the cell surface antigen Thy1, the mES markers alkaline phosphatase (AP) and SSEA1, and the self-renewal genes *Nanog* and *Oct4*. Thy1 is highly expressed in MEFs but its expression is repressed at the initiation of reprogramming. Conversely, AP and SSEA1 expression is up-regulated, followed by up-regulation of *Nanog* and endogenous *Oct4*. Thus, MEFs expressing GFP under control of *Oct4* are often used as the starting somatic cells because GFP expression then identifies cells that have been fully reprogrammed to the iPSC stage. To identify key microRNAs in reprogramming, we focused on the

early reprogramming stage in the first 5 d after transduction of MEFs with the four factors (4F; OSKM) in what is reported to be the first stage of major transcriptional changes in the biphasic reprogramming process (Polo et al. 2012). To determine whether the fate of 4F-transduced cells is set at that stage, Oct4-GFP MEFs were infected with 4F virus and then harvested 5 d later for cell sorting (Fig. 1A). PE-conjugated Thy1 antibody was used to isolate pure Thy1<sup>+</sup> and Thy1<sup>-</sup> populations, with gates set to exclude cells expressing intermediate Thy1 levels (Fig. 1B). Equal numbers (10,000 cells) of Thy1<sup>+</sup> and Thy1<sup>-</sup> cells were reseeded in 12-well plates on CF1-MEF feeders and their potential for iPSC induction was evaluated based on GFP and marker expression. Potential iPSCs were enriched mainly in the Thy1<sup>-</sup> population, as determined by counting of colonies expressing GFP or AP (Fig. 1C,D). We detected no GFP<sup>+</sup> colonies and only a few AP<sup>+</sup> colonies in the Thy1<sup>+</sup> population at Day 14 post-4F infection (Fig. 1C,E). These results suggest that the fate of 4F-infected MEFs is determined before Day 5 post-infection and that potential iPSCs are enriched in the Thy1<sup>-</sup> population. We therefore collected total RNA from sorted Thy1<sup>-</sup> cells at Day 5 post-transduction to analyze overall microRNA expression changes by microarray. To identify microRNAs whose expression is significantly altered relative to that seen in starting MEFs, we filtered the data by setting a gate of at least a twofold change in expression with  $P < 0.05$  (Fig. 1F). We identified a set of microRNAs in the Thy1<sup>-</sup> population that were significantly induced by 4F transduction (Fig. 1G). Among them, miR-135b was the most highly induced and showed a statistically significant change in expression (Supplemental Table 2 and Fig. 1A), and was thus selected for further analysis of its role, and that of its direct gene targets, in the reprogramming process. We observed that other microRNAs, such as miR-93 which belongs to the miR-25~106b cluster, miR-92a which belongs to the miR-17~92 cluster, and miR-302b which belongs to the miR-302 cluster, were also highly induced at the early stage of reprogramming, confirming previous findings (Li et al. 2011; Liao et al. 2011; Subramanyam et al. 2011). Our analysis also revealed a set of microRNAs that were significantly repressed (Fig. 1H), suggesting that they may serve as reprogramming barriers. Of these, we chose to evaluate the potential barrier function of miR-223 and miR-495, because they are highly expressed in MEFs.

### Reprogramming is enhanced by miR-135b and inhibited by miR-223 and miR-495

To determine how miR-135b affects reprogramming, miR-135b microRNA mimic was transfected into Oct4-GFP MEFs infected with 4F virus, and GFP<sup>+</sup> colonies were counted at Days 11–12 post-transduction. Transfection of the miR-135b mimic increased the number of Oct4-GFP<sup>+</sup> colonies by approximately twofold, as did transfection with miR-93, which was previously characterized as an enhancer of reprogramming (Fig. 2A; Anokye-Danso et al. 2011). In similar

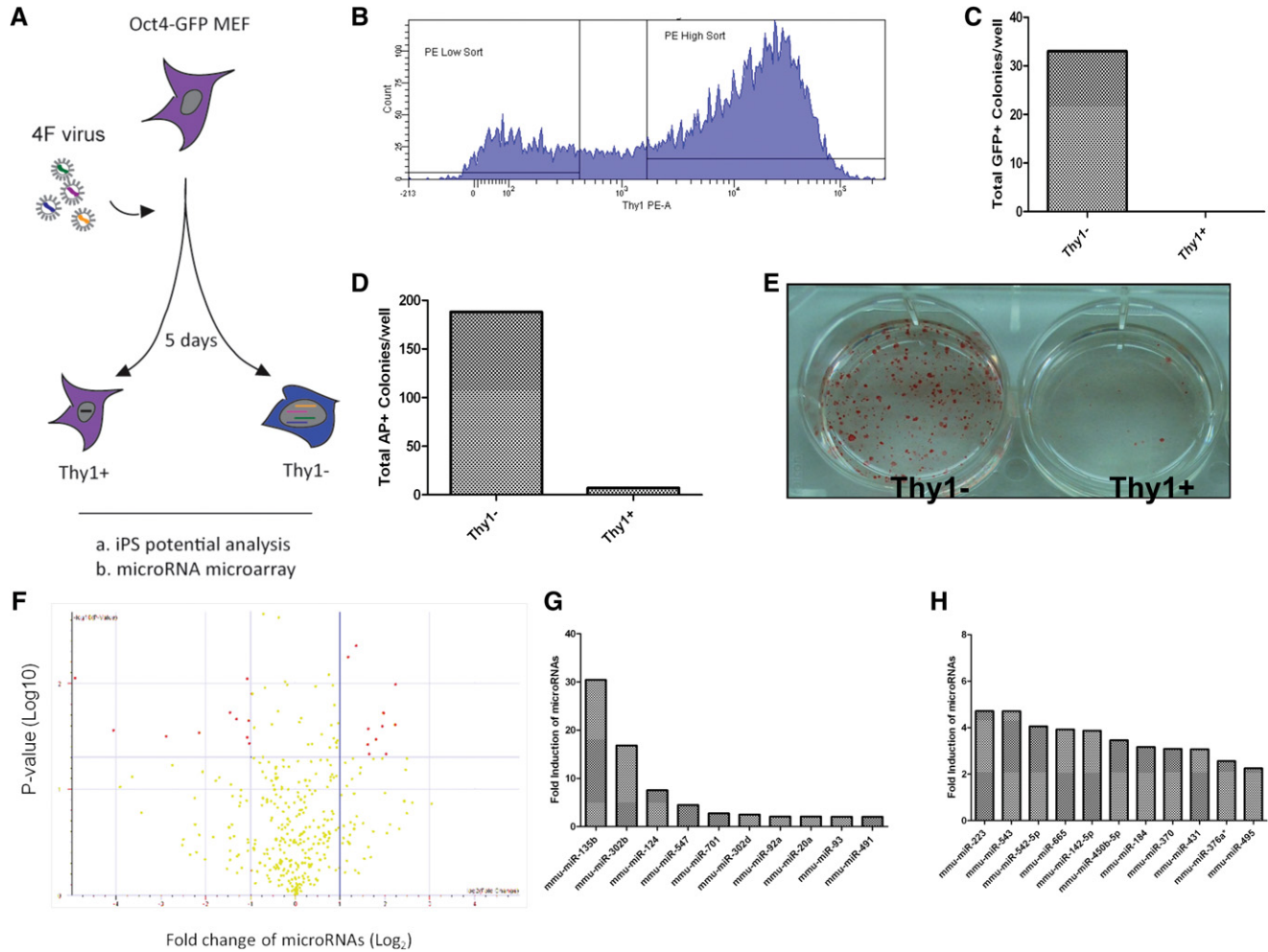


**FIGURE 1.** Identification of highly regulated microRNAs during the early reprogramming stage. (A) Scheme of experimental design. MEFs were infected with 4F virus for 5 d, and sorted based on expression of the Thy1 surface antigen. Both Thy1<sup>-</sup> and Thy1<sup>+</sup> cells were collected for microRNA expression profile analysis. (B) Representative gating for Day 5 4F-infected MEF sorting. PE-conjugated Thy1 antibody was used to detect Thy1<sup>-</sup> and Thy1<sup>+</sup> populations. (C) iPSCs were enriched in the Thy1<sup>-</sup> population of 4F-infected MEFs at Day 5. Equal numbers of cells (10,000 cells) sorted from 4F-infected MEFs were replated into feeder plates and cultured for 14 d, then GFP<sup>+</sup> colonies were counted. (D) AP staining confirmed that iPSCs generated in (C) were enriched in the Thy1<sup>-</sup> population. Cells were harvested for AP staining at Day 14 post-infection. (E) Representative image of AP<sup>+</sup> colonies from replated Thy1<sup>-</sup> and Thy1<sup>+</sup> cells. (F) Induced or repressed microRNAs were identified in Thy1<sup>-</sup> cells. Both Thy1<sup>-</sup> and Thy1<sup>+</sup> cells were harvested for microRNA expression profiling. Data from the Thy1<sup>-</sup> population were compared with the original MEFs and microRNAs showing a two-fold change and  $P < 0.05$  were identified using a volcano map. Hits are labeled as red dots. (G) Set of significantly induced microRNAs. MicroRNAs induced by at least twofold are shown. (H) Set of significantly repressed microRNAs. MicroRNAs repressed by at least twofold are shown.

experiments, cells were transfected with miR-223 or miR-495 mimics, which had minor inhibitory effects on reprogramming (Fig. 2A). This observation is potentially due to the saturation effect of endogenous miRs as these miRs already have high expression in MEFs. We then analyzed the percentage of GFP<sup>+</sup> cells in the miR-transfected reprogrammed cells and found that although both miR-93 and miR-135b increased GFP<sup>+</sup> colony formation, only miR-135b increased the overall percentage of GFP<sup>+</sup> cells by approximately twofold (Fig. 2B, Supplemental Fig. 1B). In the same assay, miR-223 transfection significantly decreased the GFP<sup>+</sup> population (Fig. 2B), supporting the possibility that it serves as a reprogramming barrier. To confirm our findings, we used microRNA inhib-

itors. As expected, blocking miR-135b compromised reprogramming efficiency, while inhibiting miR-223 resulted in a significant increase in the number of Oct4-GFP<sup>+</sup> colonies (Fig. 2C). Following transfection with miR-135b mimics or inhibitors, miR-135b expression levels were quantified by RT-qPCR to confirm overexpression or down-regulation, respectively (Supplemental Fig. 2A). Overall, these data demonstrate that miR-135b enhances reprogramming, consistent with its high induction by the 4F factors, while miR-223, which our analysis showed to be the most highly repressed microRNA, serves as a barrier.

Because GFP expression by putative iPSC could result from inappropriate reactivation of the *Oct4* locus, we asked

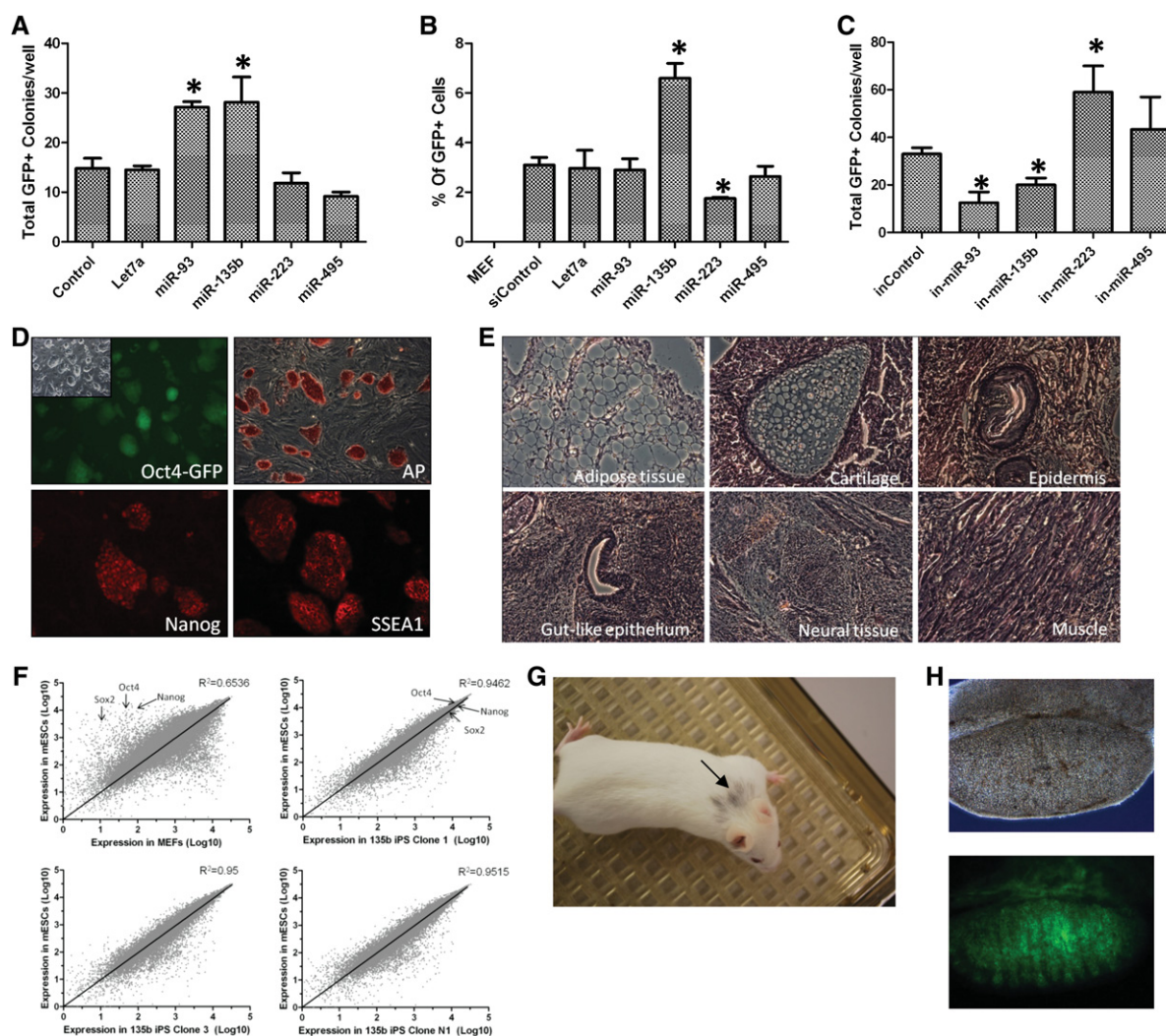


**FIGURE 2.** miR-135b enhances reprogramming of MEFs to iPSCs. (A) miR-135b enhances Oct4-GFP<sup>+</sup> colony formation. The indicated microRNA mimics were transfected at a final concentration of 50 nM into MEFs on Day 0 and again on Day 5 after 4F transduction. GFP<sup>+</sup> colonies were counted at Days 11–12. Data represent two independent experiments with triplicate wells. Let-7a was used as a control. (\*)  $P < 0.05$ . (B) miR-135b increases the percentage of Oct4-GFP<sup>+</sup> cells. Cells from the indicated treatments were harvested at Day 14 post-infection with 4F and paraformaldehyde-fixed prior to FACS analysis to determine the percentage of GFP<sup>+</sup> cells. Data represent two independent experiments with triplicate wells. (\*)  $P < 0.05$ . (C) Blocking of miR-135b compromises reprogramming. MicroRNA inhibitors were transfected into MEFs on Days 0 and 5 post-infection with 4F. GFP<sup>+</sup> colonies were counted at Days 11–12 post-infection. Data represent two independent experiments with triplicate wells. (\*)  $P < 0.05$ . (D) miR-135b iPSCs reach a fully reprogrammed state. miR-135b-transfected iPSCs were fixed with paraformaldehyde and stained for alkaline phosphatase, Nanog, and SSEA1 expression. Endogenous Oct4 expression was monitored by GFP expression. (E) Teratoma formation confirms the pluripotency of miR-135b iPSCs.  $1 \times 10^6$  iPSCs were injected into athymic nude mice and tumors were harvested for H&E staining 3–4 wk later. (F) miR-135b iPSCs show expression profiles similar to mES cells. Total RNA from miR-135b iPSCs was used for mRNA expression profile analysis and compared with original MEFs and with mES cells. The three tested miR-135b iPSC clones (clones 1, 3, and N1) showed similar expression patterns to mES cells, which were quite different from the expression profile of the original starting MEFs. (G) Chimeric mouse from miR-135b iPSC clone 4. (H) miR-135b iPSC could contribute to the germline of recipient embryos (miR-135b iPSC clone 4).

whether miR-135b-transfected iPSCs reached a fully reprogrammed state, both phenotypically and functionally. Analysis of miR-135b-transfected iPSCs indicated that they expressed appropriate markers, including AP, SSEA1, Nanog, and endogenous Oct4 (Fig. 2D). Moreover, these cells had the full capacity to differentiate into three germ layers as indicated by marker analysis (Supplemental Fig. 2B), and to form heterogeneous teratomas when injected into athymic nude

mice (Fig. 2E). Genome-wide mRNA profiling also confirmed that gene expression in miR-135b-transfected iPSCs resembled mES cells and differed significantly from MEFs (Fig. 2F), and these cells contributed to chimeric mice and showed germline transmission (Fig. 2G,H) which clearly indicated that a fully reprogrammed state has been achieved in these cells. These data demonstrated that miR-135b transfection in iPSCs did not adversely affect their pluripotency.

### Identification of miR-135b-regulated genes

We next sought to identify genes that are directly regulated by miR-135b. Initially, microRNAs were thought to simply repress mRNA translation. However, recent findings suggest that microRNA-induced degradation of mRNA is a major mechanism of mRNA repression in animals (Djuranovic et al. 2011; Huntzinger and Izaurralde 2011). Thus, we performed a genome-wide mRNA expression analysis to detect potential miR-135b targets. miR-135b or control siRNA were transfected into Oct4-GFP MEFs, and total RNAs were

harvested 48 h later for array analysis. The raw data were filtered to detect at least twofold changes in gene expression, (either increased or decreased) with  $P < 0.05$  (Fig. 3A). Candidate genes were then compared with published mESC, iPSC, and MEF expression profiles (Sridharan et al. 2009) and segregated into genes induced (group 1) or repressed (group 2) after miR-135b transfection, the latter being considered more likely to contain direct targets. Notably, we found that over 80% of the genes repressed by miR-135b transfection (group 2) were genes that are silenced as MEFs are reprogrammed to iPS/mES cells (correlated) (Fig. 3B). This was

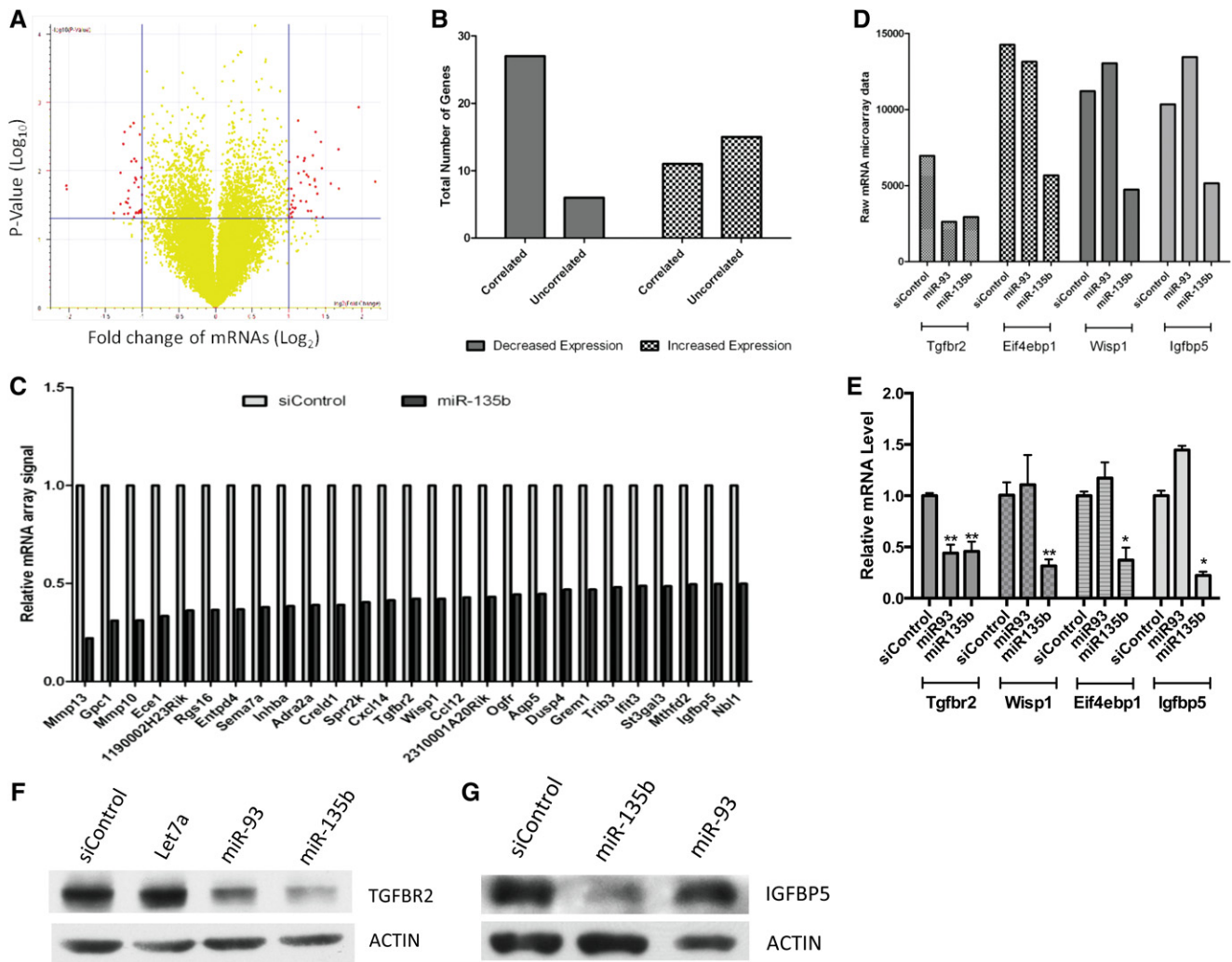


**FIGURE 3.** Genome-wide identification of potential miR-135b target genes. (A) Volcano maps from miR-135b-transfected MEFs. MEFs were transfected with siControl and miR-135b for 2 d and analyzed by mRNA expression array. Hits (red dots) were gated for at least twofold expression change and  $P < 0.05$ . (B) miR-135b-repressed genes are enriched for genes suppressed in ES/iPS cells. miR-135b-regulated genes were separated into two groups (induced or repressed) and then compared with existing iPS/ES/MEF expression profiles. “Correlated genes” indicate that genes changed upon miR-135b transfection showed similar changes from MEFs to iPS/mES cells. “Uncorrelated genes” indicate a group of genes that were changed upon miR-135b transfection but had a different (reversed) change in expression pattern from MEFs to iPS/mES cells. (C) List of correlated miR-135b-repressed genes. (D) Representative miR-135b-regulated genes from microarray. (E) Expression of miR-135b-regulated genes was confirmed by RT-qPCR. MEFs were transfected with microRNA mimics for 2 d before harvesting for RT-qPCR analysis. Error bar represents two independent experiments with duplicate samples. (F) TGFBR2 protein expression is suppressed by miR-93 and miR-135b. Total proteins were harvested for Western blotting analysis at Day 2 post-transfection with miR mimic. (G) IGFBP5 protein expression is suppressed by miR-135b. A miR-93-transfected sample was included as a negative control. RT-qPCR data was analyzed using the Wilcoxon rank-sum test. (\*)  $P < 0.05$ ; (\*\*)  $P < 0.01$ .

not observed in genes that were induced by miR-135b transfection (group 1), of which approximately half are normally suppressed during reprogramming (uncorrelated), and the other half are increased (correlated). These data suggest that miR-135b targets a subset of genes that are normally repressed during reprogramming.

To identify the targets of miR-135b, the “correlated” genes in group 1 (Fig. 3C) were analyzed using both miRanda (Enright et al. 2003) and Targetscan (Lewis et al. 2005). Potential target sites were identified based on seed region matches and overall predicted binding energy. Of 27 genes repressed by miR-135b by at least twofold, 14 contained at least one predicted miR-135b target site (Supplemental Fig. 3A and Table 1). Among them, *Wisp1*, *Tgfb2*, and *Igfbp5* showed high expression intensity detected by microarray and appeared to have direct miR-135b target sites. Therefore, they were chosen for further validation.

To confirm our mRNA microarray analysis, total RNAs were harvested from miR-135b-transfected Oct4-GFP MEFs in an independent experiment, and RT-qPCR was used to quantify the representative mRNAs. Indeed, we detected decreases in mRNA levels upon miR-135b transfection that were in good agreement with the mRNA array data (Fig. 3D, E). *Tgfb2* and *Igfbp5* mRNA levels were decreased ~70% upon miR-135b transfection, and western analysis confirmed that this was accompanied by a dramatic decrease in *Tgfb2* and *Igfbp5* protein expression (Fig. 3F,G). We cloned the 3' UTR of these potential targets into the pGL3 luciferase reporter vector and cotransfected the reporters plus the pRL-TK plasmid into HeLa cells. Indeed, miR-135b decreased luciferase activity of *Tgfb2* and *Wisp1* reporters by ~80%, and the *Igfbp5* reporter by ~30% (Supplemental Fig. 3B). We also noticed that the combination of miR-93 and 135b showed additive effects on *Tgfb2* repression (Supplemental Fig. 3C). These data strongly suggest that *Tgfb2*, *Wisp1*, and *Igfbp5* are direct targets of miR-135b, of which the latter two are key components of extracellular matrix proteins. To further validate *Wisp1* as a target of miR-135b, RT-qPCR was utilized to assess the *Wisp1* mRNA level after transfecting cells with miR-135b mimic, mutant mimic, or miR-135b inhibitors. *Wisp1* mRNA decreased by ~50% during miR mimic transfection, increased by ~25% upon inhibition and remained consistent with the nontargeting siRNA control when transfected with the mutant miR mimic (Supplemental Fig. 3D). In conjunction with the dual luciferase reporter assay, these data indicate a direct sequence specific interaction between miR-135b and *Wisp1*.

### **Wisp1 has dual roles during reprogramming and is a key regulator of ECM proteins**

We next asked whether the potential miR-135b targets *Tgfb2*, *Wisp1*, and *Igfbp5* function as reprogramming barriers. *Tgfb2* was previously reported to be a reprogramming barrier and a potential target of miR-93 and its family of microRNAs

(Li et al. 2011). In addition to *Tgfb2*, *Wisp1*, and *Igfbp5*, we chose to investigate several other genes that might be indirectly regulated by miR-135b, such as *Eif4ebp1* and *Cxcl14* as they do not have predicted miR-135b target sites. Before using siRNAs for these experiments, we confirmed by RT-qPCR that each mRNA was efficiently knocked down by at least 60% by its cognate siRNA (Fig. 4A).

To determine whether knockdown of the candidate barrier genes increased reprogramming efficiency, we transfected siRNAs into Oct4-MEFs on the same day as 4F transduction (Day 0), then again on Day 5 post-infection, and counted GFP<sup>+</sup> iPSC colonies on Days 11–12. We detected a significant increase in the number of GFP<sup>+</sup> colonies after transfection of siRNA targeting *Igfbp5* and *Tgfb2*, consistent with their possible function as barrier genes (Fig. 4B). Interestingly, a dramatic decrease in reprogramming efficiency was observed in cells transfected with siWisp1 on Days 0 and 5 post-4F infection. However, if siWisp1 was transfected on Day 5 only, there was a threefold increase in the number of GFP<sup>+</sup> colonies (Fig. 4C), suggesting that *Wisp1* can play temporally distinct roles during reprogramming. This effect was not due to a difference in siRNA transfection efficiency, because *Wisp1* mRNA knockdown was equivalent under both protocols (Fig. 4D). We observed that *Wisp1* mRNA expression was sharply reduced by 4F initially and then maintained at a steady level during the rest course of the reprogramming process (Supplemental Fig. 4A) while *Wisp1* protein levels showed a decline between Days 4 and 6 (Supplemental Fig. 4B). To analyze the significance of *Wisp1* in the context of miR-135b reprogramming, MEFs were reprogrammed while simultaneously knocking down the endogenous *Wisp1* and inhibiting miR-135b using an antisense oligo 5 d post OSKM transduction. *Wisp1* knockdown and miR-135b inhibition at Day 5 of iPS reprogramming showed an increase and a decrease in GFP<sup>+</sup> iPS colonies, respectively. However, when both were simultaneously inhibited during reprogramming, a rescuing effect in iPS Oct4-GFP-positive colonies was observed (Fig. 4E). These data suggest that *Wisp1* contributes significantly to miR-135b reprogramming and acts as a barrier to iPSC generation.

To prove this observation further, we next analyzed the effect of *Wisp1* siRNA transfection on markers of MET, which is believed to be the initial step of the reprogramming process (Li et al. 2010; Samavarchi-Tehrani et al. 2010). Remarkably, knockdown of *Wisp1* on Day 0 dramatically decreased mRNA expression of each of the MET markers tested, suggesting a significant delay or suppression of MET by siWisp1 (Fig. 4F). In contrast, *Wisp1* knockdown on Day 5 had little effect on MET marker mRNA levels, except a small and insignificant decrease in *Epcam* expression (Fig. 4G). In addition, constant overexpression of HA tagged *Wisp1* showed inhibitory effects on reprogramming (Fig. 4H) with HA-tagged *Wisp1* overexpression verified by Western blot (Supplemental Fig. 4C). Together, these data show that the role of *Wisp1* is temporally dependent, and suggest a dual role of *Wisp1* in which it acts as



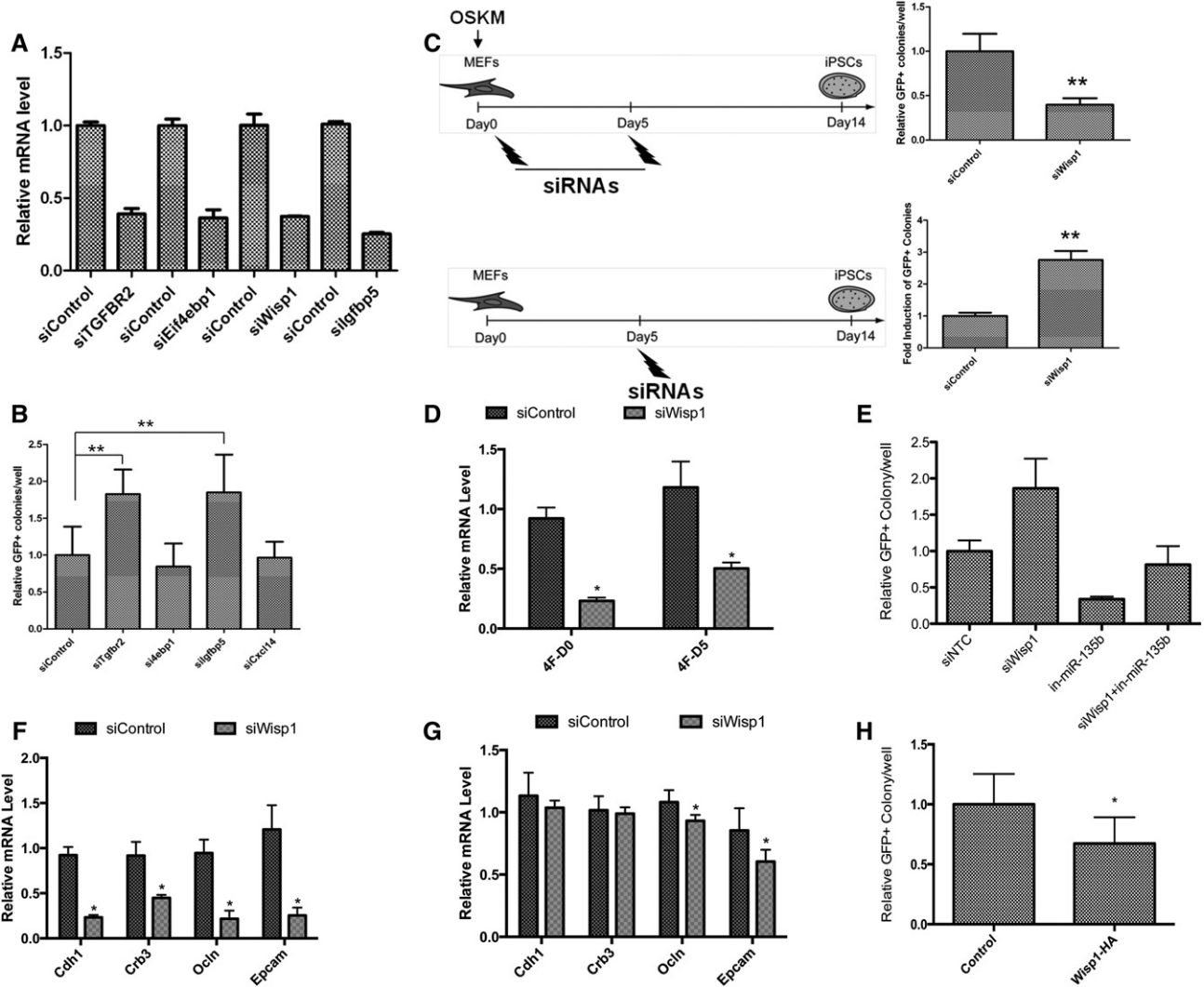


**FIGURE 4.** *Wisp1* plays a dual role during reprogramming, while *Tgfb2* and *Igfbp5* knockdown enhances reprogramming. (A) Potential target genes are efficiently knocked down by siRNAs. Smartpool siRNAs at a final concentration of 50 nM were used to transfect MEFs. Total RNAs were harvested at Day 2 for RT-qPCR to evaluate knockdown efficiency of each siRNA. (B) Knockdown of *Tgfb2* or *Igfbp5* enhances Oct4-GFP<sup>+</sup> colony formation, while knockdown of *Eif4ebp1* and *Cxcl14* had no effect. MEFs were transfected with siRNAs on Days 0 and 5 at the same time as 4F infection. GFP<sup>+</sup> colonies were counted at Days 11–12 post-infection. Error bars represent three independent experiments with triplicate wells. The *P* value was calculated using Student’s *t*-test. (\*\*) *P* < 0.01. (C) Knockdown of *Wisp1* shows stage-specific effects on reprogramming. Knockdown of *Wisp1* on the same days as 4F transduction (Day0) decreased the reprogramming efficiency by ~70%, while knockdown on Day 5 enhanced reprogramming by approximately three-fold. Error bars represent three independent experiments with triplicate wells. (\*\*) *P* < 0.01. (D) *Wisp1* is efficiently knocked down by siRNAs during both procedures. siWisp1 was transfected at a final concentration of 50 nM on Day 0 or Day 5. Total RNAs were harvested at Day 2 post-transfection for RT-qPCR analysis of *Wisp1* expression. (E) Knockdown of *Wisp1* is able to rescue iPS reprogramming after inhibition of miR-135b at Day 5. Error bars represent three independent experiments with duplicate wells. (F) Knockdown of *Wisp1* at Day 0 inhibits mesenchymal-to-epithelial transition (MET). MEFs were infected with 4F and transfected with siRNA on the same day (Day 0). Total RNAs were harvested 2 d later. Expression of several MET markers was evaluated. (G) Knockdown of *Wisp1* at Day 5 does not affect MET. MEFs were transduced with 4F at Day 0 and transfected with siRNA at Day 5 post-4F infection. Total RNAs were harvested 2 d after transfection and expression of the MET markers was evaluated. (H) Overexpression of *Wisp1* inhibits iPS induction. MEFs were transduced with a *Wisp1* HA tagged retroviral vector along with OSKM, and GFP colonies were quantified on Days 12–14. RT-qPCR data were analyzed using the Wilcoxon rank-sum test. (\*) *P* < 0.05; (\*\*) *P* < 0.01.

a positive regulator of reprogramming in the early stages and a negative regulator later.

To identify the mechanism by which *Wisp1* affects reprogramming, we next investigated the downstream targets of *Wisp1*. *Wisp1* is a member of CCN family proteins, the function of which usually includes two aspects: (1) binding of scaffold

fold of extracellular matrix proteins and (2) binding receptors and transcriptionally regulating signaling events mediated by biological active molecules such as growth factors and cytokines (Jun and Lau 2011). We reasoned that since somatic cell reprogramming is an in vitro process, it is more likely that *Wisp1* functions through transcriptional regulation of

downstream genes. To identify the downstream targets of *Wisp1*, we utilized mRNA microarrays to search for genes significantly changed upon *Wisp1* knockdown in control, non-infected and 4F-transduced MEFs (Supplemental Table 4). The microarray experiments identified a panel of ECM genes, including *Dkk2*, *Igfbp5*, *Nov*, and *Tgfb1*, that showed profoundly decreased expression upon *Wisp1* knockdown, which was confirmed by RT-qPCR (Fig. 5A). Moreover, expression of *Dkk2*, *Igfbp5*, *Nov*, and *Tgfb1* was suppressed by 4F transduction. In addition, *Wisp1* knockdown increased expression of *Ccl20* (Fig. 5A), which was also induced in MEFs by 4F transduction alone. To rule out the possibility of off-target effects of the *Wisp1* siRNA, two additional shRNAs were tested. These shRNAs efficiently suppressed *Wisp1* expression, and had the same inhibitory effects on expression of *Wisp1* target genes (Supplemental Fig. 5A). To confirm that the miR-135b effects on MEFs was at least partially mediated

through *Wisp1*, we transfected MEFs with an miR-135b mimic, and found decreased expression of *Dkk2*, *Igfbp5*, *Nov*, and *Tgfb1* (Supplemental Fig. 5B). We only observed modest up-regulation of *Wisp1* target genes with miR-135b inhibitor transfection (Supplemental Fig. 5C), possibly due to indirect targeting effects. In addition, overexpression of *Wisp1* target genes did not affect *Wisp1* expression, indicating a lack of feedback regulation (Supplemental Fig. 5D). Together, these data suggest that *Wisp1* may serve as a key regulator of ECM genes in MEFs.

To determine if expression of *Wisp1*-regulated ECM genes could affect reprogramming, Oct4-GFP MEFs were infected with 4F and on Day 5 were transfected with siRNAs targeting *Dkk2*, *Igfbp5*, *Nov*, and *Tgfb1*. Indeed, knockdown of each of these genes at Day 5 only significantly increased reprogramming efficiency (Figs. 4B, 5B), while similar biphasic effects were observed for *Tgfb1* and *Nov* when they were knocked

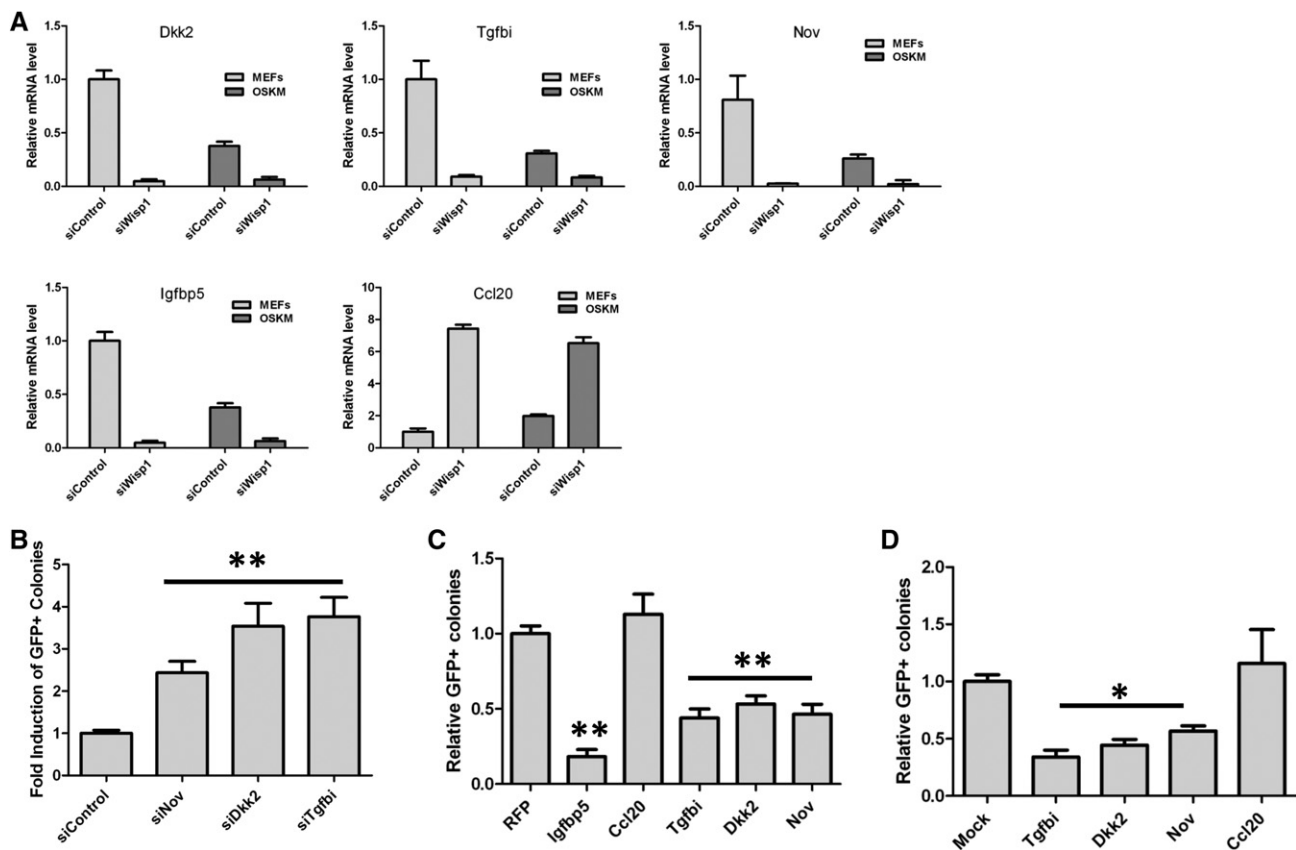


**FIGURE 5.** *Wisp1* is a key regulator of extracellular matrix genes. (A) *Wisp1* regulates expression of several ECM genes. Expression of *Tgfb1*, *Igfbp5*, *Dkk2*, *Nov*, and *Ccl20* were dramatically changed upon *Wisp1* knockdown. Uninfected and 4F-infected MEFs were transfected with siWisp1 for 2 d and total RNAs were harvested for RT-qPCR analysis of different ECM genes. Error bars represent two independent experiments with duplicate wells. (B) Knockdown of *Nov*, *Dkk2*, and *Tgfb1* significantly enhances iPSC generation. MEFs were transduced with 4F at Day 0 and transfected with siRNAs at Day 5 post-infection. GFP<sup>+</sup> colonies were quantified at around Days 11–13. Error bars represent three independent experiments with triplicate wells. (\*\*)  $P < 0.01$ . (C) Overexpression of *Wisp1*-regulated ECM genes compromises reprogramming. The indicated ECM genes were cloned into pMX retroviral vectors. MEFs were transduced with 4F plus the indicated ECM genes and GFP<sup>+</sup> colonies were quantified at around Days 11–13. Data were normalized to pMX-RFP-transduced cells. Error bars represent three independent experiments with triplicate wells. (\*\*)  $P < 0.01$ . (D) Addition of recombinant ECM proteins compromises reprogramming. Purified recombinant TGFBI, DKK2, NOV, and CCL20 were added at a final concentration of 100 ng/mL to cultures of 4F-MEFs undergoing reprogramming. GFP<sup>+</sup> colonies were quantified at Days 11–13. Error bars represent two independent experiments with triplicate wells. (\*)  $P < 0.05$ .

down at Days 0 and 5 (Supplemental Fig. 6A). We also detected an increase in mES marker gene expression in the siRNA-transfected cells (Supplemental Fig. 6B). Conversely, overexpression of these genes in MEFs strongly reduced GFP<sup>+</sup> colony formation, particularly with *Igfbp5*, which reduced reprogramming by ~70% (Fig. 5C). Interestingly, addition of recombinant DKK2, TGFBI, and NOV proteins to the 4F-transfected MEF cultures from Day 5 post infection had similar effects on the cells as overexpression of the genes (Fig. 5D), demonstrating that the effects of *Wisp1* were mediated by secretion of the protein products of its target genes,

and confirming that the *Wisp1*-regulated ECM genes do indeed act as barriers to the reprogramming process.

Based on the results described above, we propose a model of how *Wisp1* may have a biphasic effect on MEF reprogramming (Fig. 6A). *Wisp1* is highly and specifically expressed in MEFs compared with iPSCs (Sridharan et al. 2009), and through its effects on the downstream ECM genes, plays a crucial role in maintaining normal MEF growth. This is supported by our finding that persistent knockdown of *Wisp1* and *Nov* (Supplemental Fig. 7A) by shRNAs in MEFs compromises their proliferation (Supplemental Fig. 7B). shRNA mediated

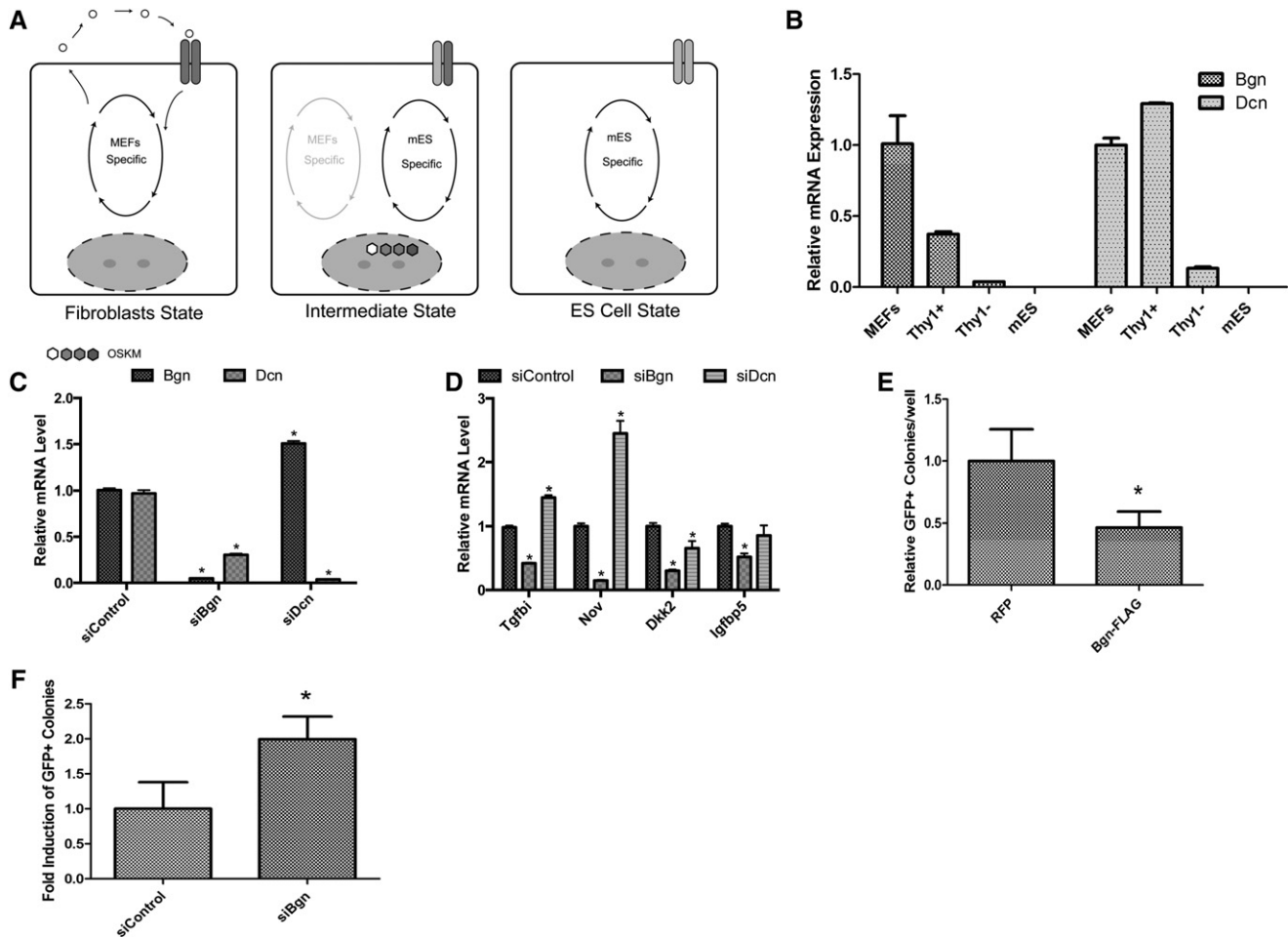


**FIGURE 6.** Target gene regulation by *Wisp1* through biglycan. (A) Proposed model for *Wisp1* dual role during reprogramming. In wild-type MEFs (fibroblast state), normal proliferation and function of the cells are dependent on a MEF-specific regulation network, where *Wisp1* is one of the most important ECM components and regulates the expression of several other ECM genes. In 4F-transduced MEFs (intermediate state), two systems co-exist; one from the MEF-specific network and the other from the four transcription factors. ECM signals from the MEF-specific network interfere with the cells becoming fully reprogrammed. In fully reprogrammed cells (ES cell state), ECM receptors are no longer expressed, and the cells are thus resistant to interfering signals from surrounding MEFs. (B) Biglycan and decorin are specifically expressed in MEFs. Expression of biglycan and decorin was analyzed by RT-qPCR in sorted cells. (C) Biglycan and decorin are efficiently knocked down by siRNAs. MEFs were transfected with siRNAs for 2 d and total RNAs were harvested for RT-qPCR analysis. (D) Knockdown of biglycan decreases expression of *Wisp1*-regulated ECM genes. Expression of *Wisp1*-regulated ECM genes was analyzed in MEFs subjected to knockdown of biglycan or decorin. Error bars represent two independent experiments with duplicate wells. (E) Overexpression of biglycan inhibits reprogramming. Flag-tagged biglycan was cloned into pMX vector and transduced into MEFs together with 4F. GFP<sup>+</sup> colonies were quantified at Days 11–13. Error bar represents two independent experiments with triplicate wells. (\*)  $P < 0.05$ . (F) Knockdown of biglycan enhances reprogramming. Biglycan siRNAs were transfected into MEFs at Day 5 post-4F transduction. GFP<sup>+</sup> colonies were quantified at Days 11–13. Error bar represents two independent experiments with triplicate wells. RT-qPCR data were analyzed using the Wilcoxon rank-sum test. (\*)  $P < 0.05$ .

knockdown of *Wisp1* also confirms a similar biphasic effect on reprogramming (Supplemental Fig. 7C). siRNA-mediated knockdown of *Nov* also showed impaired cell proliferation (Supplemental Fig. 7E). Upon 4F transduction and reprogramming, infected MEFs would have two regulatory networks, one established by the four reprogramming factors, and the other being endogenous. The ability of a cell to become fully reprogrammed would depend on whether the 4F-induced network could silence the existing MEF regulatory network. In these cells, although MEF-specific genes such as *Wisp1* and its potential receptors are being down-regulated, the remaining receptors could still be stimulated by signals secreted by surrounding cells that are not reprogrammed. This constant stimulation of the original MEF network would compete with the 4F-mediated ES regulatory network and resulted in a low efficiency for cells to become fully reprogrammed. Thus, knocking down *Wisp1* in these cells could reduce the MEF signaling stimulation, significantly break the balance, and push them toward a fully reprogrammed state. Once the cells become mES-like cells, MEF ECM genes and receptors are completely shut down and they become resistant to the signals from nearby feeder cells.

### **Wisp1 may regulate ECM genes through its interaction with biglycan**

To test our model (Fig. 6A), we searched the literature for known factors that could interact with *Wisp1*. If our model is correct, we predict we will see high expression of these genes in the starting population of MEFs, whereas cells undergoing reprogramming will down-regulate but not extinguish their expression, and expression will be silenced in fully reprogrammed iPSCs/mES cells. Interestingly, *Wisp1* has been reported to bind the proteoglycans decorin and biglycan on the surface of human skin fibroblasts (Desnoyers et al. 2001) and both are highly expressed in MEFs (Sridharan et al. 2009). To determine if decorin and biglycan might be involved in *Wisp1* regulation in MEFs, we first examined their gene expression in the starting MEFs, the sorted *Thy1*<sup>+/-</sup> cells, and in mES populations. The two genes were highly expressed in MEFs but undetectable in mES cells (Fig. 6B). They were highly expressed in *Thy1*<sup>+</sup> cells and showed strongly reduced but detectable expression in *Thy1*<sup>-</sup> cells (Fig. 6B), which are enriched in potential iPSCs (Fig. 1C–E). We then transfected MEFs with siRNAs targeting these two genes and confirmed the knockdown efficiency by RT-qPCR (Fig. 6C). Of interest, knockdown of *biglycan* also decreased *decorin* expression, suggesting possible cross regulation of the two genes. Knockdown of *biglycan* also decreased the expression of the *Wisp1* target genes *Dkk2*, *Igfbp5*, *Nov*, and *Tgfb1*, to a similar level to that seen with *Wisp1* knockdown (Fig. 6D). Consistent with these observations, overexpression of *biglycan* strongly suppressed reprogramming, and conversely, knockdown significantly enhanced reprogramming (Fig. 6E,F). In addition, we also observed a similar phenotype with *decorin* knockdown

and overexpression (Supplemental Fig. 8). Therefore, we conclude that biglycan may be an intermediate for *Wisp1*-mediated regulation of ECM genes.

### **DISCUSSION**

Since the discovery that MEFs can be directly reprogrammed to iPSCs, considerable effort has been made to understand how the four reprogramming transcription factors extinguish endogenous MEF gene expression and gradually reestablish mES-like regulatory networks. Understanding the critical barriers to reprogramming is essential to allow development of novel technologies and compounds to improve the efficiency and to elucidate the underlying transcriptional and epigenetic changes associated with the pluripotent state. Here, we used microRNAs as powerful tools to dissect the molecular mechanisms that elicit successful reprogramming. We analyzed a *Thy1*<sup>-</sup> cell population enriched in potential iPSCs to identify its microRNA expression profile during the early stages of reprogramming. From these experiments, we identified sets of microRNAs that were induced or repressed during the process, and showed that manipulating their expression with miR mimics or inhibitors dramatically altered the efficiency of iPSC induction. Among the microRNAs analyzed, miR-135b was the most highly induced by the four factors, and was shown to enhance iPSC generation. Moreover, by mining genome-wide mRNA expression data for potential miR-135b target genes, we showed that *Wisp1* and its downstream ECM genes could compromise the efficiency of the reprogramming process. Therefore, our approach has not only identified a novel ECM network that is involved in modulating the reprogramming process, but we have also shown that using microRNAs as probes could be an efficient method to study both the intracellular and extracellular molecular mechanisms of reprogramming.

Somatic cell reprogramming is believed to be a stochastic process in which extensive gene network rewiring happens within the reprogramming cells (Hanna et al. 2009). According to the previous report on molecular cornerstones of the reprogramming process (Stadtfield et al. 2008), the reprogramming factors are only needed during the initial 8 d for cells to become fully reprogrammed. One of the most notable changes in the transition from somatic to embryonic stem cell-like identity is the modulated expression of cell surface antigens. According to previous reports and our own studies, the transition from *Thy1*<sup>+</sup> to *Thy1*<sup>-</sup> represents an important early step, where most of the potential iPSCs are present in the *Thy1*<sup>-</sup> population, and significant transcriptional changes occur (Polo et al. 2012). In this study, we identified miR-135b to be among the most highly induced microRNAs during this key *Thy1*<sup>+</sup> to *Thy1*<sup>-</sup> transitional stage and showed that its putative extracellular matrix targets, particularly *Wisp1*, act as barriers to the reprogramming process.

*Wisp1* was first described as a Wnt1-inducible protein (Pennica et al. 1998). It belongs to the CCN gene family

that encodes six 30–40 kDa secreted proteins (Chen and Lau 2009; Berschneider and Konigshoff 2011). CCN proteins have four conserved structural domains with sequences homologous to insulin-like growth factor binding proteins (IGFBPs), von Willebrand factor type C repeat (VWC), thrombospondin type I repeat (TSP), and carboxyl-terminal (CT) domain. These domains determine the function of CCN member proteins during development and in human diseases. Although *Wisp1* has been linked to oncogenic transformation (Pennica et al. 1998; Xu et al. 2000), proliferation and cell survival (Venkatachalam et al. 2009; Venkatesan et al. 2010), and epithelial-to-mesenchymal transition (Konigshoff et al. 2009), little is known about its downstream genes or how it regulates their expression. In this study, we identified several downstream ECM components that were regulated by *Wisp1*, likely through its interaction with biglycan. These include *Tgfbi*, *Dkk2*, *Igfbp5*, and *Nov*. These findings provide some new insights into *Wisp1* function. For example, *Tgfbi* is a known downstream gene induced by TGF $\beta$  signaling and has profound tumor suppressive effects (Ahmed et al. 2007; Zhang et al. 2009). The TGF $\beta$  signaling pathway has itself been identified as a barrier for somatic reprogramming (Ichida et al. 2009; Maherali and Hochedlinger 2009). Our finding thus indicates there may be crosstalk between *Wisp1* and TGF $\beta$  signaling in regulating expression of the ECM protein TGFBI. Knockdown of *Wisp1* decreases *Tgfbi* expression, which might compromise TGF $\beta$  signaling and allow cells to become fully reprogrammed. Two other *Wisp1* target genes we identified are *DKK2* and *IGFBP5*. *DKK2* is known as a Wnt signaling antagonist (Kawano and Kypta 2003), and *IGFBP5* could regulate IGF signaling by binding to IGF-1/2 (Beattie et al. 2006). We found that knockdown of *Wisp1* decreased expression of *Dkk2* and *Igfbp5*, which would derepress Wnt and IGF signaling. Consistent with this, previous studies have indicated that Wnt signaling could promote somatic reprogramming (Marson et al. 2008). It was recently shown that *IGFBP5* overexpression induces cell senescence in a p53-dependent manner (Kim et al. 2007). This protein is highly expressed in fibroblasts, and its expression is further increased upon senescence (Yoon et al. 2004). Thus, decreased expression of *IGFBP5* and *DKK2* is likely to be beneficial to iPSC generation. Furthermore, it was recently reported that Wnt signaling also regulates iPSC reprogramming in a stage-specific manner in which Wnt inhibits early stage reprogramming but enhances it later (Hou et al. 2013). Our findings are consistent with this biphasic effect and suggest that the Wnt signal pathway may be an underlying or overlapping mechanism in our proposed extracellular matrix regulated model.

Over the past few years much progress has been made in understanding the molecular mechanisms of somatic reprogramming, and several important barrier pathways have been discovered. However, these efforts have mainly focused on intracellular signaling networks, and the effect of the extracellular environment on reprogramming has not been fully ex-

plored. In our study, biglycan, a surface glycoprotein that binds *Wisp1*, is expressed in MEFs but decreases in reprogramming cells, as shown in *Thy1*<sup>-</sup> cells that are enriched with potential iPSCs. These cells will still be stimulated by *Wisp1* and presumably other ECM proteins secreted by surrounding feeder MEF cells or unprogrammed cells, as they still express the receptors such as biglycan, although at much lower level compared with original MEFs. These stimulations would prevent the cells from shutting down MEF-specific regulation networks and compete with four factors-mediated regulatory networks to determine the fate of target cells. Meanwhile, our discovery that microRNAs induced by the four factors can regulate ECM genes reveals some new insights into how the four factors manage to reprogram a small percentage of cells. Down-regulation of MEF-specific ECM proteins seems to be part of the entire reprogramming process and is mediated at least in part by 4F-mediated induction of microRNAs such as miR-135b. Together with previous findings, it is clear that microRNAs are important regulators of reprogramming, both through intracellular and extracellular mechanisms (Fig. 7).

In summary, we have identified a novel microRNA-mediated pathway of ECM gene regulation that is involved in iPSC generation. Our results indicate that 4F-induced miR-135b expression in turn regulates expression of *Wisp1* and *Igfbp5*. *Wisp1* is a key regulator of several ECM proteins, which may be mediated through *Wisp1* interaction with biglycan. Our findings not only identify a novel role for ECM components in somatic cell reprogramming, but also demonstrate that microRNAs can be powerful tools to dissect the intracellular and extracellular molecular mechanisms of iPSC generation.

## MATERIALS AND METHODS

### Cell culture, vectors, and virus transduction

Oct4-GFP MEFs were derived from mouse embryos harboring an IRES-EGFP fusion cassette downstream from the stop codon of *pou5f1* (Jackson lab, Stock#008214) at E13.5. MEFs were cultured in DMEM (Invitrogen, 11995-065) with 10% FBS (Invitrogen) plus glutamine and nonessential amino acids (NEAA). Only MEFs at passage 0–4 were used for iPSC induction. pMXs-Oct4, Sox2, Klf4, and cMyc were purchased from Addgene. *Tgfbi*, *Dkk2*, *Igfbp5*, *Nov*, and biglycan overexpression vectors were constructed by inserting cDNA coding sequences into the pMX vector. To generate retrovirus, PLAT-E cells were seeded in 10 cm plates. The next day, the cells were transfected with 9  $\mu$ g of each vector using Lipofectamine (Invitrogen, 18324-012) and PLUS (Invitrogen, 11514-015). Viruses were harvested and combined 2 d later. For iPSC induction, MEFs were seeded in 12-well plates and the next day were transduced with “four factor” (4F) virus with 4  $\mu$ g/mL Polybrene. One day later, the medium was changed to fresh MEF medium, and 3 d later it was changed to mES culture medium supplemented with LIF (Millipore, ESG1107). GFP<sup>+</sup> colonies were picked at Day 14 post-transduction, and expanded clones were

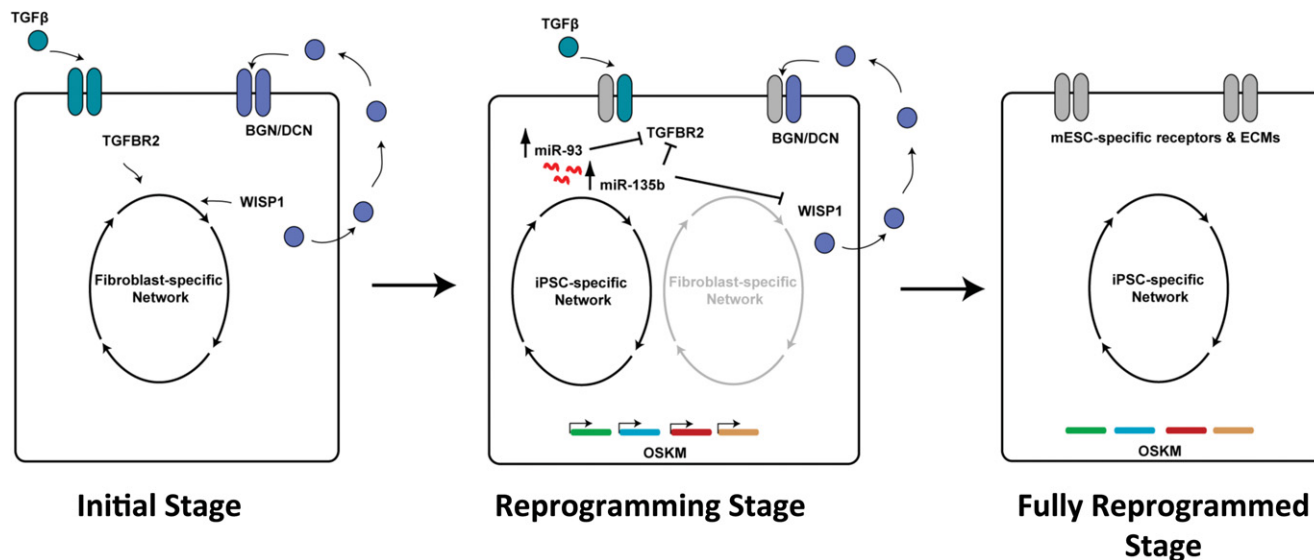


**FIGURE 7.** Model for roles of microRNAs during the reprogramming process. MicroRNAs induced by the four factors regulate intracellular and extracellular processes involved in cell fate decisions. Intracellularly, microRNAs target signaling pathways that are barriers for iPSC generation, such as TGF $\beta$  signaling, the p53–p21 pathway, and cell cycle control. Meanwhile, some microRNAs, such as miR-135b, regulate expression of ECM genes to establish a growth environment that promotes the fully reprogrammed state. Both groups of microRNAs work collaboratively following 4F transduction to reprogram MEFs to iPSCs.

cultured in DMEM with 15% FBS (Hyclone) plus LIF, thioglycerol, glutamine, and NEAA. Irradiated CF1 MEFs served as feeder cells to culture mES and derived iPSC clones.

Recombinant proteins were obtained from commercial sources as follows: mouse Dkk2 (R&D systems, 2435DK/CF), human NOV/CCN3 (R&D systems, 1640NV), human TGFBI (Prospec, #PRO-568), CCL20 (R&D systems, 760-M3).

### MicroRNAs, siRNAs, and MEF transfection

microRNA mimics and inhibitory siRNAs were purchased from Dharmacon. To transfect MEFs, microRNA mimics were diluted in Opti-MEM (Invitrogen, 11058-021) to the desired final concentration. Lipofectamine 2000 (Invitrogen, 11668-019) (2  $\mu$ L/well) was added and the mixture was incubated for 20 min at RT. For 12-well plate transfections, 80  $\mu$ L of the miR mixture was added to each well with 320  $\mu$ L of Opti-MEM. Three hours later, 0.8 mL of the virus mixture (for iPSC) or fresh medium was added to each well, and the medium was changed to fresh MEF medium the next day.

### Western blotting

Total cell lysates were prepared using M-PER buffer (PIERCE, 78503), incubated on ice for 20 min, and cleared by centrifuging at 13,000 rpm for 10 min. Equal amounts of lysate were loaded onto 10% SDS-PAGE gels. Proteins were transferred to PVDF membranes (Bio-Rad, 1620177) using the semidry system (Bio-Rad) and then blocked with 5% milk in Tris-buffered saline–Tween 20 (TBST: 50 mM Tris, 150 mM NaCl, 0.05% Tween20) for at least 1 h at room temperature or overnight at 4°C. The following antibodies were used: anti-mNanog (R&D Systems, AF2729), anti-h/mSSEA1 (R&D Systems, MAB2156), anti-TGFBR2 (Cell Signaling, #3713), anti-IGFBP5 (R&D Systems, AF578), anti-actin (Thermo, MS1295P0),

anti-AFP (Abcam, ab7751), anti- $\beta$  III tubulin (R&D Systems, MAB1368), anti-WISP1 (Santa Cruz Biotechnology, sc-25441), and anti- $\alpha$  actinin (Sigma, A7811).

### Expression data analysis

Illumina Mouse\_miRNA-12 v2 and Illumina Mouse-6 v2 Expression BeadChips were analyzed using the manufacturers BeadArray Reader and primary data were collected using the supplied Scanner software. Data analysis was done in three stages. First, expression intensities were calculated for each gene probed on the array for all hybridizations using Illumina's Beadstudio3 software. Second, intensity values were quality controlled and normalized using the Illumina Beadstudio detection with a  $P$ -value threshold set to  $<0.05$ , thus removing genes which were effectively absent from the array. The initial 379 miRNAs were reduced to 368 following this step. All the arrays were then normalized using the normalize.quantiles routine from the Affy package in Bioconductor. This procedure accounted for any variation in hybridization intensity between the individual arrays. An assessment of several different normalization techniques using the Bioconductor maCorrPlot routine suggested that normalize.quantiles was the most appropriate for the data.

Finally, these normalized data were imported into GeneSpring and analyzed for differentially expressed miRNAs. The groups of biological replicates were included in the analysis, and significantly differentially expressed genes were determined on the basis of  $t$ -tests and fold difference changes in expression level.

The initial comparison was between the MEF samples (two biological replicates) and the Thy1<sup>-</sup> samples (two biological replicates). Differentially expressed miRNAs were determined by searching for miRNAs with statistically significant differences between the groups based on the results of the Welch  $t$ -test (parametric test, variances not assumed equal;  $P$ -value cutoff 0.05). This yielded a list of 9–22 genes out of the initial 379. To find the genes with the most

robust changes in expression, the data were plotted as a “Volcano Plot” (see Fig. 1), which allows statistical significance to be measured along with the extent of fold change in expression. Hence, the outliers are those genes with the highest fold change which is also statistically significant.

### mRNA and microRNA RT and quantitative PCR

Total RNAs were extracted using Trizol (Invitrogen), and then 1 µg total RNA was used for RT using Superscript II (Invitrogen). Quantitative PCR was performed using a Roche LightCycler480 II and the SYBR Green mixture from Abgene (Ab-4166). Mouse Ago2, Dicer, Drosha, Gapdh, and p21 primers are defined in Supplemental Table 2. Other primers were described previously (Takahashi and Yamanaka 2006). For microRNA quantitative analysis, total RNA was extracted using the method described above. Between ~1.5 and 3 µg of total RNA was used for microRNA reverse transcription using the QuantiMir kit following the manufacturer’s protocol (System BioSciences, RA420A-1). RT products were then used for quantitative PCR using the mature microRNA sequence as a forward primer and the universal primer provided with the kit. RT-qPCR data were analyzed using the nonparametric Wilcoxon rank-sum test. (\*)  $P < 0.05$ ; (\*\*)  $P < 0.01$ ; (\*\*\*)  $P < 0.001$ .

### Immunostaining

Cells were washed twice with PBS and fixed with 4% paraformaldehyde at room temperature for 20 min. Fixed cells were permeabilized with 0.1% Triton X-100 for 5 min, and then blocked in 5% BSA in PBS containing 0.1% Triton X-100 for 1 h at room temperature. Primary antibody was diluted at 1:100 to 1:400 in 2.5% BSA PBS containing 0.1% Triton X-100, according to the manufacturer’s protocol. Cells were stained with primary antibody for 1 h and then washed three times with PBS. Secondary antibody was diluted 1:400, and cells were stained for 45 min at room temperature.

### Embryoid body formation and differentiation assay

iPSCs were trypsinized to a single cell suspension, and the hanging drop method was used to generate embryoid bodies (EB). For each drop, 4000 iPSCs in 20 µL EB differentiation medium were used. EBs were cultured in hanging drops for 3 d before being reseeded onto gelatin-coated plates. After reseeded, cells were cultured until Day 14, when apparent beating areas could be identified.

### Teratoma formation

To generate teratomas, iPSCs were trypsinized and resuspended at a concentration of  $1 \times 10^7$  cells/mL. Athymic nude mice were anesthetized with Avertin, and 150 µL of iPSCs were injected into each mouse. Tumors were monitored every week for ~3–4 wk. Tumors were then harvested and fixed in Z-Fix solution for 24 h at room temperature, before paraffin embedding, sectioning, and H&E staining. To further evaluate pluripotency of derived iPSC clones, iPSCs were injected into C57BL/6J-Tyr(C-2J)/J (albino) blastocysts. Generally, each blastocyst received 12–18 iPSCs. ICR recipient females were used for embryo transfer.

## SUPPLEMENTAL MATERIAL

Supplemental material is available for this article.

## ACKNOWLEDGMENTS

We thank members of the Rana laboratory for helpful discussions and support. We thank the following shared resource facilities at the Sanford-Burnham Institute: Genomics, Informatics and Data Management Core for miRNA and mRNA array experiments and data analysis; Animal Facility for the generation of teratomas and chimeric mice; and the Histology and Molecular Pathology Core for characterization of various tissues. This work was supported in part by the National Institutes of Health. The manuscript has been seen and approved by all authors.

Received December 9, 2013; accepted August 27, 2014.

## REFERENCES

- Adams JC, Watt FM. 1993. Regulation of development and differentiation by the extracellular matrix. *Development* **117**: 1183–1198.
- Ahmed AA, Mills AD, Ibrahim AE, Temple J, Blenkinsop C, Vias M, Massie CE, Iyer NG, McGeoch A, Crawford R, et al. 2007. The extracellular matrix protein TGFBI induces microtubule stabilization and sensitizes ovarian cancers to paclitaxel. *Cancer Cell* **12**: 514–527.
- Ambros V. 2004. The functions of animal microRNAs. *Nature* **431**: 350–355.
- Anokye-Danso F, Trivedi CM, Juhr D, Gupta M, Cui Z, Tian Y, Zhang Y, Yang W, Gruber PJ, Epstein JA, et al. 2011. Highly efficient miRNA-mediated reprogramming of mouse and human somatic cells to pluripotency. *Cell Stem Cell* **8**: 376–388.
- Banito A, Rashid ST, Acosta JC, Li S, Pereira CF, Geti I, Pinho S, Silva JC, Azuara V, Walsh M, et al. 2009. Senescence impairs successful reprogramming to pluripotent stem cells. *Genes Dev* **23**: 2134–2139.
- Beattie J, Allan GJ, Lochrie JD, Flint DJ. 2006. Insulin-like growth factor-binding protein-5 (IGFBP-5): a critical member of the IGF axis. *Biochem J* **395**: 1–19.
- Bendall SC, Stewart MH, Menendez P, George D, Vijayaragavan K, Werbowetski-Ogilvie T, Ramos-Mejia V, Rouleau A, Yang J, Bosse M, et al. 2007. IGF and FGF cooperatively establish the regulatory stem cell niche of pluripotent human cells in vitro. *Nature* **448**: 1015–1021.
- Berschneider B, Konigshoff M. 2011. WNT1 inducible signaling pathway protein 1 (WISP1): a novel mediator linking development and disease. *Int J Biochem Cell Biol* **43**: 306–309.
- Bissell MJ, Hines WC. 2011. Why don’t we get more cancer? A proposed role of the microenvironment in restraining cancer progression. *Nat Med* **17**: 320–329.
- Brambrink T, Foreman R, Welstead GG, Lengner CJ, Wernig M, Suh H, Jaenisch R. 2008. Sequential expression of pluripotency markers during direct reprogramming of mouse somatic cells. *Cell Stem Cell* **2**: 151–159.
- Carey BW, Markoulaki S, Hanna JH, Faddah DA, Buganim Y, Kim J, Ganz K, Steine EJ, Cassidy JP, Creighton MP, et al. 2011. Reprogramming factor stoichiometry influences the epigenetic state and biological properties of induced pluripotent stem cells. *Cell Stem Cell* **9**: 588–598.
- Chen CC, Lau LF. 2009. Functions and mechanisms of action of CCN matrix proteins. *Int J Biochem Cell Biol* **41**: 771–783.
- Choi YJ, Lin CP, Ho JJ, He X, Okada N, Bu P, Zhong Y, Kim SY, Bennett MJ, Chen C, et al. 2011. miR-34 miRNAs provide a barrier for somatic cell reprogramming. *Nat Cell Biol* **13**: 1353–1360.
- Chu CY, Rana TM. 2006. Translation repression in human cells by microRNA-induced gene silencing requires RCK/p54. *PLoS Biol* **4**: e210.

- Chu CY, Rana TM. 2007. Small RNAs: regulators and guardians of the genome. *J Cell Physiol* **213**: 412–419.
- Desnoyers L, Arnott D, Pennica D. 2001. WISP-1 binds to decorin and biglycan. *J Biol Chem* **276**: 47599–47607.
- Djuranovic S, Nahvi A, Green R. 2011. A parsimonious model for gene regulation by miRNAs. *Science* **331**: 550–553.
- Enright AJ, John B, Gaul U, Tuschl T, Sander C, Marks DS. 2003. MicroRNA targets in *Drosophila*. *Genome Biol* **5**: R1.
- Guo S, Zi X, Schulz VP, Cheng J, Zhong M, Koochaki SH, Megyola CM, Pan X, Heydari K, Weissman SM, et al. 2014. Nonstochastic reprogramming from a privileged somatic cell state. *Cell* **156**: 649–662.
- Hanna J, Saha K, Pando B, van Zon J, Lengner CJ, Creighton MP, van Oudenaarden A, Jaenisch R. 2009. Direct cell reprogramming is a stochastic process amenable to acceleration. *Nature* **462**: 595–601.
- Henzler CM, Li Z, Dang J, Arcila ML, Zhou H, Liu J, Chang KY, Bassett DS, Rana TM, Kosik KS. 2013. Staged miRNA re-regulation patterns during reprogramming. *Genome Biol* **14**: R149.
- Hong H, Takahashi K, Ichisaka T, Aoi T, Kanagawa O, Nakagawa M, Okita K, Yamanaka S. 2009. Suppression of induced pluripotent stem cell generation by the p53–p21 pathway. *Nature* **460**: 1132–1135.
- Hou P, Li Y, Zhang X, Liu C, Guan J, Li H, Zhao T, Ye J, Yang W, Liu K, et al. 2013. Pluripotent stem cells induced from mouse somatic cells by small-molecule compounds. *Science* **341**: 651–654.
- Huntzinger E, Izaurralde E. 2011. Gene silencing by microRNAs: contributions of translational repression and mRNA decay. *Nat Rev Genet* **12**: 99–110.
- Ichida JK, Blanchard J, Lam K, Son EY, Chung JE, Egli D, Loh KM, Carter AC, Di Giorgio FP, Koszka K, et al. 2009. A small-molecule inhibitor of  $\text{tgf-}\beta$  signaling replaces *sox2* in reprogramming by inducing nanog. *Cell Stem Cell* **5**: 491–503.
- Jiao J, Dang Y, Yang Y, Gao R, Zhang Y, Kou Z, Sun XF, Gao S. 2013. Promoting reprogramming by FGF2 reveals that the extracellular matrix is a barrier for reprogramming fibroblasts to pluripotency. *Stem Cells* **31**: 729–740.
- Judson RL, Babiarczyk JE, Venere M, Belloch R. 2009. Embryonic stem cell-specific microRNAs promote induced pluripotency. *Nat Biotechnol* **27**: 459–461.
- Jun JI, Lau LF. 2011. Taking aim at the extracellular matrix: CCN proteins as emerging therapeutic targets. *Nat Rev Drug Discov* **10**: 945–963.
- Kawamura T, Suzuki J, Wang YV, Menendez S, Morera LB, Raya A, Wahl GM, Belmonte JC. 2009. Linking the p53 tumour suppressor pathway to somatic cell reprogramming. *Nature* **460**: 1140–1144.
- Kawano Y, Kypta R. 2003. Secreted antagonists of the Wnt signalling pathway. *J Cell Sci* **116**: 2627–2634.
- Kessenbrock K, Plaks V, Werb Z. 2010. Matrix metalloproteinases: regulators of the tumor microenvironment. *Cell* **141**: 52–67.
- Kim KS, Seu YB, Baek SH, Kim MJ, Kim KJ, Kim JH, Kim JR. 2007. Induction of cellular senescence by insulin-like growth factor binding protein-5 through a p53-dependent mechanism. *Mol Biol Cell* **18**: 4543–4552.
- Kim NH, Kim HS, Li XY, Lee I, Choi HS, Kang SE, Cha SY, Ryu JK, Yoon D, Fearon ER, et al. 2011. A p53/miRNA-34 axis regulates Snail1-dependent cancer cell epithelial-mesenchymal transition. *J Cell Biol* **195**: 417–433.
- Konigshoff M, Kramer M, Balsara N, Wilhelm J, Amarie OV, Jahn A, Rose F, Fink L, Seeger W, Schaefer L, et al. 2009. WNT1-inducible signaling protein-1 mediates pulmonary fibrosis in mice and is upregulated in humans with idiopathic pulmonary fibrosis. *J Clin Invest* **119**: 772–787.
- Lewis BP, Burge CB, Bartel DP. 2005. Conserved seed pairing, often flanked by adenosines, indicates that thousands of human genes are microRNA targets. *Cell* **120**: 15–20.
- Li MA, He L. 2012. microRNAs as novel regulators of stem cell pluripotency and somatic cell reprogramming. *Bioessays* **34**: 670–680.
- Li Z, Rana TM. 2012. A kinase inhibitor screen identifies small-molecule enhancers of reprogramming and iPS cell generation. *Nat Commun* **3**: 1085.
- Li H, Collado M, Villasante A, Strati K, Ortega S, Canamero M, Blasco MA, Serrano M. 2009. The *Ink4/Arf* locus is a barrier for iPS cell reprogramming. *Nature* **460**: 1136–1139.
- Li R, Liang J, Ni S, Zhou T, Qing X, Li H, He W, Chen J, Li F, Zhuang Q, et al. 2010. A mesenchymal-to-epithelial transition initiates and is required for the nuclear reprogramming of mouse fibroblasts. *Cell Stem Cell* **7**: 51–63.
- Li Z, Yang CS, Nakashima K, Rana TM. 2011. Small RNA-mediated regulation of iPS cell generation. *EMBO J* **30**: 823–834.
- Liao B, Bao X, Liu L, Feng S, Zovoilis A, Liu W, Xue Y, Cai J, Guo X, Qin B, et al. 2011. MicroRNA cluster 302–367 enhances somatic cell reprogramming by accelerating a mesenchymal-to-epithelial transition. *J Biol Chem* **286**: 17359–17364.
- Lipchina I, Elkabetz Y, Hafner M, Sheridan R, Mihailovic A, Tuschl T, Sander C, Studer L, Betel D. 2011. Genome-wide identification of microRNA targets in human ES cells reveals a role for miR-302 in modulating BMP response. *Genes Dev* **25**: 2173–2186.
- Lowry WE, Richter L, Yachechko R, Pyle AD, Tchieu J, Sridharan R, Clark AT, Plath K. 2008. Generation of human induced pluripotent stem cells from dermal fibroblasts. *Proc Natl Acad Sci* **105**: 2883–2888.
- Maherali N, Hochedlinger K. 2009.  $\text{Tgf}\beta$  signal inhibition cooperates in the induction of iPSCs and replaces *Sox2* and *cMyc*. *Curr Biol* **19**: 1718–1723.
- Marson A, Foreman R, Chevalier B, Bilodeau S, Kahn M, Young RA, Jaenisch R. 2008. Wnt signaling promotes reprogramming of somatic cells to pluripotency. *Cell Stem Cell* **3**: 132–135.
- Melton C, Judson RL, Belloch R. 2010. Opposing microRNA families regulate self-renewal in mouse embryonic stem cells. *Nature* **463**: 621–626.
- Miyoshi N, Ishii H, Nagano H, Haraguchi N, Dewi DL, Kano Y, Nishikawa S, Tanemura M, Mimori K, Tanaka F, et al. 2011. Reprogramming of mouse and human cells to pluripotency using mature microRNAs. *Cell Stem Cell* **8**: 633–638.
- Nakagawa M, Koyanagi M, Tanabe K, Takahashi K, Ichisaka T, Aoi T, Okita K, Mochizuki Y, Takizawa N, Yamanaka S. 2008. Generation of induced pluripotent stem cells without *Myc* from mouse and human fibroblasts. *Nat Biotechnol* **26**: 101–106.
- Nichols J, Silva J, Roode M, Smith A. 2009. Suppression of Erk signalling promotes ground state pluripotency in the mouse embryo. *Development* **136**: 3215–3222.
- Park IH, Zhao R, West JA, Yabuuchi A, Huo H, Ince TA, Lerou PH, Lensch MW, Daley GQ. 2008. Reprogramming of human somatic cells to pluripotency with defined factors. *Nature* **451**: 141–146.
- Peerani R, Rao BM, Bauwens C, Yin T, Wood GA, Nagy A, Kumacheva E, Zandstra PW. 2007. Niche-mediated control of human embryonic stem cell self-renewal and differentiation. *EMBO J* **26**: 4744–4755.
- Pennica D, Swanson TA, Welsh JW, Roy MA, Lawrence DA, Lee J, Brush J, Taneyhill LA, Deuel B, Lew M, et al. 1998. WISP genes are members of the connective tissue growth factor family that are up-regulated in wnt-1-transformed cells and aberrantly expressed in human colon tumors. *Proc Natl Acad Sci* **95**: 14717–14722.
- Pfaff N, Fiedler J, Holzmann A, Schambach A, Moritz T, Cantz T, Thum T. 2011. miRNA screening reveals a new miRNA family stimulating iPS cell generation via regulation of *Meox2*. *EMBO Rep* **12**: 1153–1159.
- Polo JM, Anderssen E, Walsh RM, Schwarz BA, Nefzger CM, Lim SM, Borkent M, Apostolou E, Alaei S, Cloutier J, et al. 2012. A molecular roadmap of reprogramming somatic cells into iPS cells. *Cell* **151**: 1617–1632.
- Qin H, Diaz A, Blouin L, Lebbink RJ, Patena W, Tanbun P, LeProust EM, McManus MT, Song JS, Ramalho-Santos M. 2014. Systematic identification of barriers to human iPS cell generation. *Cell* **158**: 449–461.
- Rais Y, Zviran A, Geula S, Gafni O, Chomsky E, Viukov S, Mansour AA, Caspi I, Krupalnik V, Zerbib M, et al. 2013. Deterministic direct reprogramming of somatic cells to pluripotency. *Nature* **502**: 65–70.
- Rana TM. 2007. Illuminating the silence: understanding the structure and function of small RNAs. *Nat Rev Mol Cell Biol* **8**: 23–36.



- Rozario T, DeSimone DW. 2010. The extracellular matrix in development and morphogenesis: a dynamic view. *Dev Biol* **341**: 126–140.
- Sakurai K, Talukdar I, Patil VS, Dang J, Li Z, Chang KY, Lu CC, Delorme-Walker V, Dermardirossian C, Anderson K, et al. 2014. Kinome-wide functional analysis highlights the role of cytoskeletal remodeling in somatic cell reprogramming. *Cell Stem Cell* **14**: 523–534.
- Samavarchi-Tehrani P, Golipour A, David L, Sung HK, Beyer TA, Datti A, Woltjen K, Nagy A, Wrana JL. 2010. Functional genomics reveals a BMP-driven mesenchymal-to-epithelial transition in the initiation of somatic cell reprogramming. *Cell Stem Cell* **7**: 64–77.
- Sanes JR. 1989. Extracellular matrix molecules that influence neural development. *Annu Rev Neurosci* **12**: 491–516.
- Silva J, Barrandon O, Nichols J, Kawaguchi J, Theunissen TW, Smith A. 2008. Promotion of reprogramming to ground state pluripotency by signal inhibition. *PLoS Biol* **6**: e253.
- Sridharan R, Tchieu J, Mason MJ, Yachechko R, Kuoy E, Horvath S, Zhou Q, Plath K. 2009. Role of the murine reprogramming factors in the induction of pluripotency. *Cell* **136**: 364–377.
- Stadtfeld M, Maherali N, Breault DT, Hochedlinger K. 2008. Defining molecular cornerstones during fibroblast to iPSC cell reprogramming in mouse. *Cell Stem Cell* **2**: 230–240.
- Subramanyam D, Lamouille S, Judson RL, Liu JY, Bucay N, Derynck R, Blesch R. 2011. Multiple targets of miR-302 and miR-372 promote reprogramming of human fibroblasts to induced pluripotent stem cells. *Nat Biotechnol* **29**: 443–448.
- Takahashi K, Yamanaka S. 2006. Induction of pluripotent stem cells from mouse embryonic and adult fibroblast cultures by defined factors. *Cell* **126**: 663–676.
- Takahashi K, Tanabe K, Ohnuki M, Narita M, Ichisaka T, Tomoda K, Yamanaka S. 2007. Induction of pluripotent stem cells from adult human fibroblasts by defined factors. *Cell* **131**: 861–872.
- Utikal J, Polo JM, Stadtfeld M, Maherali N, Kulalert W, Walsh RM, Khalil A, Rheinwald JG, Hochedlinger K. 2009. Immortalization eliminates a roadblock during cellular reprogramming into iPSCs. *Nature* **460**: 1145–1148.
- Venkatachalam K, Venkatesan B, Valente AJ, Melby PC, Nandish S, Reusch JE, Clark RA, Chandrasekar B. 2009. WISP1, a pro-mitogenic, pro-survival factor, mediates tumor necrosis factor- $\alpha$  (TNF- $\alpha$ )-stimulated cardiac fibroblast proliferation but inhibits TNF- $\alpha$ -induced cardiomyocyte death. *J Biol Chem* **284**: 14414–14427.
- Venkatesan B, Prabhu SD, Venkatachalam K, Mummidi S, Valente AJ, Clark RA, Delafontaine P, Chandrasekar B. 2010. WNT1-inducible signaling pathway protein-1 activates diverse cell survival pathways and blocks doxorubicin-induced cardiomyocyte death. *Cell Signal* **22**: 809–820.
- Warren L, Manos PD, Ahfeldt T, Loh YH, Li H, Lau F, Ebina W, Mandal PK, Smith ZD, Meissner A, et al. 2010. Highly efficient reprogramming to pluripotency and directed differentiation of human cells with synthetic modified mRNA. *Cell Stem Cell* **7**: 618–630.
- Wernig M, Meissner A, Foreman R, Brambrink T, Ku M, Hochedlinger K, Bernstein BE, Jaenisch R. 2007. In vitro reprogramming of fibroblasts into a pluripotent ES-cell-like state. *Nature* **448**: 318–324.
- Xu L, Corcoran RB, Welsh JW, Pennica D, Levine AJ. 2000. WISP-1 is a Wnt-1- and  $\beta$ -catenin-responsive oncogene. *Genes Dev* **14**: 585–595.
- Yang C-S, Rana TM. 2013. Learning the molecular mechanisms of the reprogramming factors: Let's start from microRNAs. *Mol Biosyst* **9**: 10–17.
- Yang CS, Li Z, Rana TM. 2011a. microRNAs modulate iPSC cell generation. *RNA* **17**: 1451–1460.
- Yang CS, Lopez CG, Rana TM. 2011b. Discovery of nonsteroidal anti-inflammatory drug and anticancer drug enhancing reprogramming and induced pluripotent stem cell generation. *Stem Cells* **29**: 1528–1536.
- Yang CS, Chang KY, Rana TM. 2014. Genome-wide functional analysis reveals factors needed at the transition steps of induced reprogramming. *Cell Rep* **8**: 327–337.
- Ying QL, Wray J, Nichols J, Battle-Morera L, Doble B, Woodgett J, Cohen P, Smith A. 2008. The ground state of embryonic stem cell self-renewal. *Nature* **453**: 519–523.
- Yoon IK, Kim HK, Kim YK, Song IH, Kim W, Kim S, Baek SH, Kim JH, Kim JR. 2004. Exploration of replicative senescence-associated genes in human dermal fibroblasts by cDNA microarray technology. *Exp Gerontol* **39**: 1369–1378.
- Yu J, Vodyanik MA, Smuga-Otto K, Antosiewicz-Bourget J, Frane JL, Tian S, Nie J, Jonsdottir GA, Ruotti V, Stewart R, et al. 2007. Induced pluripotent stem cell lines derived from human somatic cells. *Science* **318**: 1917–1920.
- Zhang Y, Wen G, Shao G, Wang C, Lin C, Fang H, Balajee AS, Bhagat G, Hei TK, Zhao Y. 2009. TGFBI deficiency predisposes mice to spontaneous tumor development. *Cancer Res* **69**: 37–44.
- Zhu S, Wei W, Ding S. 2011. Chemical strategies for stem cell biology and regenerative medicine. *Annu Rev Biomed Eng* **13**: 73–90.